Domain wall motion and precursor dynamics in $PbZrO_3$

S. Puchberger[1],* V. Soprunyuk[1], A. Majchrowski[2], K. Roleder[3], and W Schranz[1]†
[1] *University of Vienna, Faculty of Physics, Boltzmanngasse 5, A-1090 Wien, Austria*
[2] *Institute of Applied Physics, Military University of Technology, ul. Kaliskiego 2, 00-908 Warsaw, Poland and*
[3] *Institute of Physics, University of Silesia, ul. Uniwersytecka 4, 40-007 Katowice, Poland*
(Dated: August 1, 2016)

Single crystals of $PbZrO_3$ have been studied by Dynamic Mechanical Analysis measurements in the low frequency range f=0.02 - 50 Hz. The complex Young's modulus exhibits a quite rich behaviour and depends strongly on the direction of the applied dynamic force. In pseudocubic $[100]_c$-direction we found intrinsic elastic behaviour as expected from Landau theory: At the antiferroelectric transition $T_c \approx 510$ K a downwards cusp anomaly in Y' accompanied by a peak in Y'' points to a quadratic/linear order parameter/strain coupling in the Landau free energy. Both anomalies are increasing with decreasing frequency showing that the measurements are performed in the limit $\omega\tau_{th} \gg 1$. Frequency scans around T_c indicate that this dispersion originates from heat-diffusion dynamics, which leads to a crossover from isothermal to adiabatic elastic behaviour in this low frequency regime. Above T_c we observe a pronounced precursor softening, quite similar as it was found in other perovskites, which can be perfectly fitted including isotropic order parameter fluctuations.
The low frequency elastic response in $[110]_c$-direction is different. Below T_c we find in addition to the intrinsic anomaly a strong contribution from ferroelastic domains, which leads to an additional softening in Y'. With decreasing temperatures this superelastic softening gradually disappears, due to an increasing relaxation time τ_{DW} for domain wall motion. From frequency dependent measurements of $Y''(T,f)$ a Vogel-Fulcher like temperature dependence of τ_{DW} was found, indicating glassy behaviour of domain freezing in $PbZrO_3$. In contrast to the $[100]_c$-direction, for forces along $[110]_c$ we found a pronounced precursor hardening, starting at about 60 K above T_c. Since this anomaly is of dynamic nature, starting at the same temperature as the observed birefringence and piezoelectric anomalies [Ko, *et al.* Phys. Rev. B **87**, 184110 (2013)], we conclude that it originates from slow dynamic polar clusters that couple to strain.

PACS numbers: 77.80.-e, 77.80.Dj, 62.40.+i, 64.70.K-

I. INTRODUCTION

After decades of damnation domains and domain walls became objects of increasing interest in physics and materials science. There are several reasons for this growing importance. On the one hand it was discovered that domains in ferroic or multiferroic materials can be tailored to tune materials properties in a desired way by so called "domain-geometry-engineering"[1]. In such samples the spatial distribution of domains is tuned to adapt to the wave-vectors of applied electric, optical or acoustic fields giving rise to a qualitatively new kind of response which is specified by the symmetry of the multidomain system. With increasing number of the domains the response of the sample to external fields is roughly described by tensorial properties averaged over all of the domain states S_i (i=1,...,n) involved. The symmetry group H which describes the corresponding macroscopic tensor properties of a so called "domain-average-engineered" crystal is the point group consisting of symmetry elements that leave all domain states $\{S_1, ..., S_n\}$ invariant. Very interesting effects occur if the domains get smaller and smaller, e.g. due to a decrease of domain wall energy, or even above T_c when they appear as dynamics precursor fluctuations. It was shown that micro- or nano - domains can adapt very easily to external boundary conditions and relax under external forces if pinning is weak[2]. Such adaptive microstructures play important roles in a large number of quite different systems, i.e. in martensitic alloys (e.g. Cu-Au)[3], in ferroelectric or ferroelastic systems with low domain wall energies[2,3], etc. Such a dense system of domains and domain walls can lead to a giant macroscopic response. One of the first examples, showing the influence of domain wall motion to the dielectric permittivity was KH_2PO_4 (KDP)[4]. The contribution from the motion of N ferroelectric domains to the permittivity was originally calculated by Kittel[5] as

$$\epsilon^{DW} \propto \frac{NP_s^2}{q} \tag{1}$$

Quite generally the number N of domain walls, the spontaneous polarization P_s as well as the restoring force q can depend on temperature T, making it challenging to calculate the domain wall contribution quantitatively for a given system. Moreover, a finite measurement frequency changes the domain wall response drastically[6,7]. In some cases "freezing" of the domain wall motion occurs at lower temperatures T_f where the domain walls can no longer follow the dynamically applied external force. As a result the susceptibility falls down to a value which corresponds to the domain-averaged limit. Prominent examples, in which such a behaviour was found in dielectric measurements are e.g. KDP[8] and TGS[9]. Domain walls have also been shown to play an important

role in ferroelastic materials. In $SrTiO_3$ the domain wall contribution to the elastic susceptibility is largely exceeding the intrinsic elastic anomaly[10], which is due to the couplings between the order parameter and the strains. Interestingly enough, no domain freezing was observed[11] in $SrTiO_3$ down to the lowest measured T=6 K. Domain wall induced elastic softening, so called "superelastic softening" was found over the years in many proper and improper ferroelastic materials, e.g. $KMnF_3$[12,13], $Ca_{1-x}Sr_xTiO_3$[14], $LaAlO_3$[15], $La_{1-x}Nd_xP_5O_{14}$[16], etc. In most of these materials domain freezing occurs at $T_f < T_c$. A similarity of domain wall dynamics and glass behaviour was already noticed some time ago in ferroelectric materials like KDP and TGS[17]. The authors proposed a model of pinning of randomly distributed defects to domain walls (DW's), which becomes increasingly collective at low temperatures, thereby restricting the motion of DW's. In a recent paper Kumar, *et al.*[18] reported an electric field - induced transition between locally pinned (rather strong glass-former) and clustered (super-fragile glass-former) phases of domain-wall-matter in KDP. Ren, *et al.*[19,20] found evidence for so called "strain glass" behaviour in TiNi-based alloys. The authors found a crossover from a normal martensitic transition to a strain glass behaviour by point defect doping in the Ti_{50-x} Ni_{50+x} system, around $x_c \approx 1.1$ where x is the concentration of point defects (excess Ni). Ren concluded that strain glass is the glass form of a ferroelastic/martensitic system due to point defect doping. He mentioned the striking similarity between strain glass and ferroelectric relaxor and cluster spin glass that leads to the concept of ferroic glass. However, recently criticism on the existence of "strain glasses"[21] appeared, giving room for further studies. Salje, *et al.*[22] proposed the existence of glasses in ferroelastic systems, appearing without the need of any defects. They called it "domain glass". The basic idea[23] is that the domain boundaries generate the defects intrinsically and at a certain density of domain walls jamming leads to a Vogel-Fulcher type slowing down of the dynamics around T_{VF}.

There are not many systems where Vogel-Fulcher dynamics was unambiguously detected for ferroelastic domains. In one of the best studied systems, $LaAlO_3$, a clear Arrhenius behaviour was found from very detailed Dynamic Mechanical Analysis measurements[15]. The opportunity to study the physics of glasses in domain wall systems brought us on the track to study the movement of domain walls in $PbZrO_3$ (PZO). Lead Zirconate exhibits a phase transition[24–26] from a paraelectric phase with cubic symmetry $Pm\bar{3}m$ (Z=1) to an antiferroelectric orthorhombic phase $Pbam$ (Z=8) at $T_c \approx 503 - 510$ K, depending on crystal quality. The orthorhomic unit cell is related to the cubic system (Fig.1) with $\mathbf{a}_c$=a_c(1,0,0), $\mathbf{b}_c$=a_c(0,1,0), $\mathbf{c}_c$=a_c(0,0,1) as $\mathbf{a}_o$=$\mathbf{a}_c$−$\mathbf{b}_c$, $\mathbf{b}_o$=2($\mathbf{a}_c$+$\mathbf{b}_c$) and $\mathbf{c}_o$=2$\mathbf{c}_c$, with orthorhombic lattice parameters given as a_o=5.876 Å $\approx \sqrt{2}a_c$, b_o=11.771 Å $\approx 2\sqrt{2}a_c$ and c_o=8.219 Å $\approx 2a_c$, since a_c=4.1597 Å[27].

Although Lead Zirconate was regarded as a model antiferroelectric crystal[28], a theoretical model to explain the transition turned out to be far from being easy. There is general agreement that the antiferroelectric phase transition in PZO is driven by an interplay of several modes[29,30], and not simply by a zone-boundary mode as would be expected in analogy to e.g. ferroelectric transitions that occur in the BZ-center.

In addition, PZO attracted special attention due to the existence of polar clusters in the high temperature cubic phase. These polar micro- or nanoregions occur as a result of anharmonic Pb ion hopping[31] which leads to a coupling of soft optic and acoustic phonon modes above T_c[32]. According to this model the polar cluster dynamics sets in far above T_c at about $T^* \approx 1.1T_c$ and they grow rapidly on approaching T_c from the cubic phase[32,33]. Such precursor phenomena present in AFE PZO are suggested to be common to perovskite ferroelectrics[33] and have indeed been observed in many other perovskite oxides[34–36]. Ko et al.[37] studied precursor effects in PZO and inferred that polar clusters grow upon cooling in a temperature range of $\sim 80°C$ above T_c and show up as a finite birefringence and piezoelectric coefficient above the structural instability. Salje, *et al.*[2,22] argued that such precursors can form glassy states leading to a Vogel-Fulcher type elastic softening[38].

In the present paper we report detailed results of Dynamic Mechanical Analysis (DMA) measurements of single crystals $PbZrO_3$ in the low frequency regime (f=0.05 - 50 Hz) in the temperature range from 220 - 580 K. In section II we give an overview about the growth and preparation of $PbZrO_3$ single crystals and the DMA-method. The results are presented in section III and they are discussed in section IV.

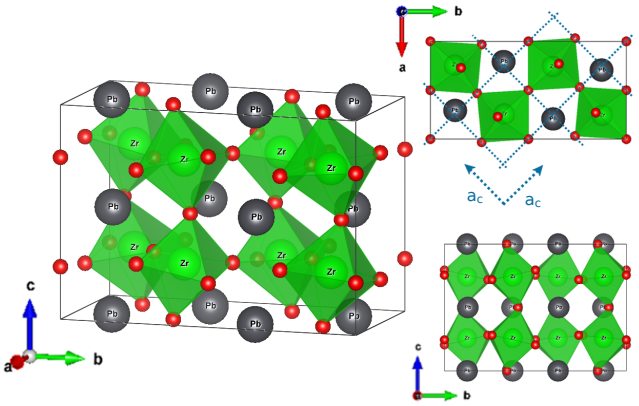

FIG. 1. Crystal structure of $PbZrO_3$ in orthorhombic $Pbam$ phase. The pseudocubic unit cell is indicated by blue dotted lines in the upper right figure.

II. EXPERIMENTAL

Pure lead zirconate, because of its incongruent melting, has to be grown by a high-temperature solution

growth (flux) method. Mainly spontaneous crystallization is used. The resulting crystals can be divided into three groups. The first group of crystals have a good performance for optical studies (thin plates) but a relatively high electrical conductivity, so these crystals are not suitable for testing of electrical and electromechanical properties. Another attempt at growing of crystals was taken in order to decrease their electrical conductivity. Relatively large dark crystals were obtained with very good electrical properties. Unfortunately, dark and large crystals were not good enough to study the optical properties (e.g. birefringence). To obtain crystals of both high optical quality and good electrical properties we used self-flux containing lead oxide and small amounts of B_2O_3 to diminish evaporation of the solvent and extend the temperature range of crystallization. Boron ions did not contaminate growing crystals due to big differences in ionic radii and different valency compared to Pb and Zr ions. Instead of PbO we used pure Pb_3PO_4 as a source of lead ions, contrary to most of the previous works. Its content was matched in molar ratio to pure PbO. Oxidizing properties of this mixed lead compound had positive influence on optical as well as electrical properties of as-grown crystals. The detailed description of PZO crystallization can be found in Ref.29.

The low frequency elastic measurements were performed with a Dynamic Mechanical Analyser (Diamond DMA, Perkin Elmer). We used "parallel plate geometry" (PP) where the sample is placed between two parallel plates and subject to a static force F_{stat} with an additional smaller dynamic force F_{dyn} whose frequency can be varied between f=0.01 - 100 Hz. The DMA registers the amplitude u and phase shift δ between applied force and amplitude via a linear variable differential transformer (LVDT), which is used to calculate the real and imaginary part of the samples Young's modulus $Y^* = Y' + iY''$

$$Y^*(\mathbf{p}) = \frac{h}{u}\frac{F_{\rm dyn}}{A} exp(i\delta) \qquad (2)$$

where h denotes the sample thickness, A its area and $\mathbf{p}$ denotes the direction of the applied force, with respect to the crystal axes. For $\mathbf{p}$ in $[100]_c$- and $[110]_c$-direction the Young's modulus can be written in cubic phase as

$$Y_{[100]} = (C_{11} - C_{12})\frac{C_{11} + 2C_{12}}{C_{11} + C_{12}} \qquad (3)$$
$$Y_{[110]} = 2(C_{11} - C_{12})\frac{C_{11} + 2C_{12}}{C_{11}}$$

Using the values of elastic constants at T_c+151 K (and at about T_c), recently measured with Brillouin Scattering[39], i.e. C_{11}=212.3 GPa (180.3 GPa) and $C_{11}-C_{12}$=143,2 GPa (125.2 GPa), we find that the magnitudes of $Y_{[100]}$ and $Y_{[110]}$ as well as their temperature dependencies in cubic phase are to main extent determined by $C_{11} - C_{12}$. In the orthorhombic phase the Young's modulus includes a combination of additional elastic constants, getting even more complicated when domains are involved.

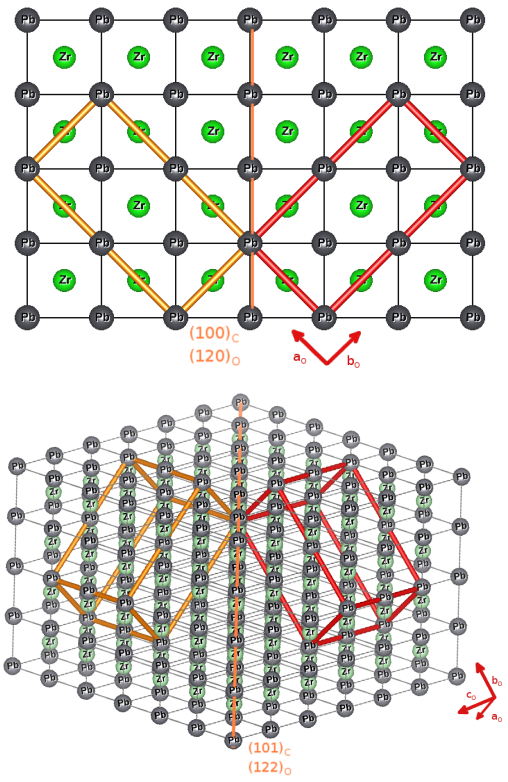

FIG. 2. Models of domain walls in AFE orthorombic phase of $PbZrO_3$. The 90° domain boundary sited on $(100)_c$, corresponding to $(120)_o$, plane and 60° domain boundary sited on $(101)_o$, corresponding to $(122)_c$ plane. The coordinate systems label the axis directions of the orthorombic cell. (Note that oxygen atoms have been omitted in these images for simplicity.)

In previous electron microscopy studies of the domain structure of PZO[48] two different types of domain configurations corresponding to 90° and 60° domains were observed in the orthorhombic phase. Figure 2 sketches the 90° and 60° domains and the corresponding domain boundaries. As the polarization direction is parallel to $\mathbf{a}_o$ its direction is switched by 90° in case of 90° domains with the domain wall being a pseudo-cubic $\{100\}_c$. If the polarization direction is switched by 60° in a $\{101\}_c$ this plane is referred to as 60° domain wall. Such 60° domains are transformed to each other by rotation around a $\langle 111\rangle_c$ axis by 120°.

The dimensions of the two measured samples were A $\approx$ 5 mm^2 ($\approx$ 2.3 mm^2) and h $\approx$ 3 mm ($\approx$ 1.8 mm). The resolution of the apparatus is $\Delta u \approx 10$ nm and $\Delta\delta \approx 0.1°$. Although the relative accuracy of DMA measurements is within 0.2-1%, the absolute accuracy is usually not better than about 20%. For this reason all plots here are shown in terms of normalized Young's modulus $Y'_n = Y'/Y'_{\rm para}$ and $Y''_n = Y'_n \tan(\delta)$, where $Y'_{\rm para}$ is the saturation value of the Young's modulus in the cubic phase.

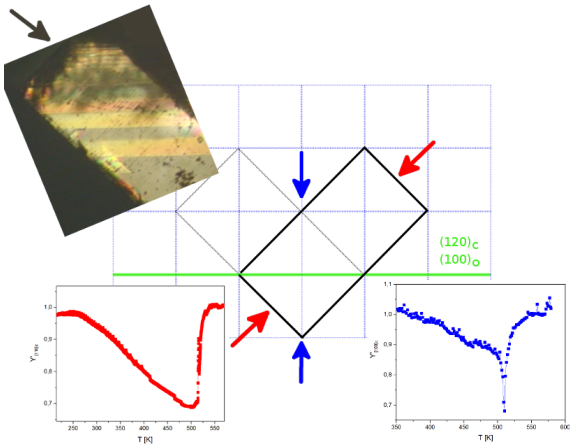

FIG. 3. Sketch of the geometrical situation and elastic response for two different directions of applied force (red and blue arrows) during a parallel plate measurement of a $PbZrO_3$ crystal containing two domain states and a domain wall (green line) oriented in $[010]_o$-direction, corresponding to $[1\bar{2}0]_c$. Top left image shows a polarized light microscopy image of the measured sample with domain walls. The black arrow indicates the direction of applied force during the measurement of $Y_{[110]c}$, corresponding to red arrows in sketch.

A more detailed description of this method and its application for the study of phase transitions is given in Refs. 40 and 41.

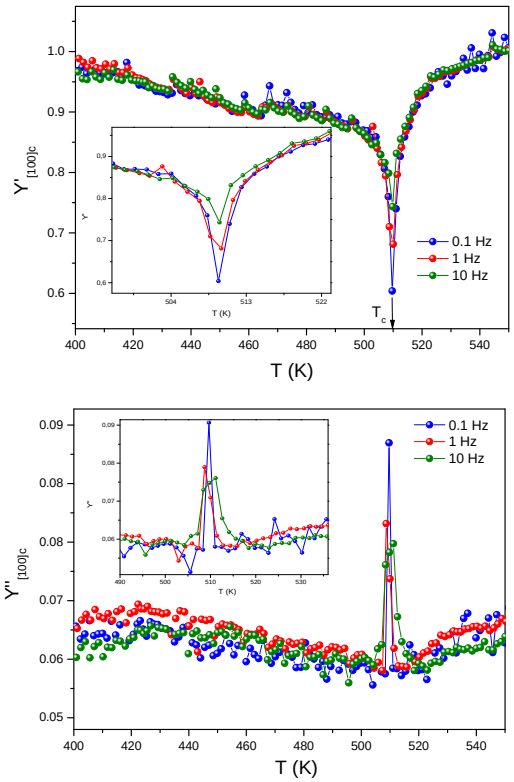

FIG. 4. Temperature dependencies of real and imaginary parts of Young's modulus of $PbZrO_3$ measured in $[100]_c$-direction at various frequencies. Insets show magnifications near the phase transition.

III. RESULTS

A. Domain wall motion - domain freezing

Temperature and frequency dependent DMA measurements of $PbZrO_3$ single crystals with forces applied in two different directions (Fig.3) are presented in the following figures. Figure 4 shows real ($Y'_{[100]c}$) and imaginary ($Y''_{[100]c}$) parts of the Young's modulus measured along one of the main cubic crystallographic axes. In this direction the force is perpendicular to the domain walls orientations and as a result the elastic anomaly resembles the intrinsic behaviour (right plot in Fig.3).

A pronounced softening of the elastic constant is already detected in the cubic phase, followed by a dip in $Y'_{[100]c}$ and a peak in $Y''_{[100]c}$ at T_c. Both anomalies decrease with increasing frequency. It is evident that the decrease of both anomalies with increasing frequency implies that $\omega\tau_{\rm sl} \gtrsim 1$, leading to $\tau_{\rm th} \approx 1$ s.

A quite different pattern is found (Fig.5) when the applied force is rotated by 45° to measure $Y_{[110]c}$, as shown in Fig.3. Instead of the narrow dip in Y' of Fig.4 a broad softening is now detected in this direction which is accompanied by a broad peak in Y'' much below the narrow peak at T_c. With increasing frequency the peak maximum of the broad peak shifts to higher temperatures. It is quite evident that the low frequency elastic behaviour in this direction is dominated by domain wall motion that induces the additional softening[10,11]. At sufficiently low frequencies the domain walls can follow the externally applied stress as long as the characteristic relaxation time $\tau_{\rm DW}$ for DW movement is small enough, leading to an efficient "superelastic softening". With decreasing temperature $\tau_{\rm DW}$ increases and the DW's can no longer follow the applied stress, implying that the elastic response turns back to the domain averaged value. To analyse the underlying dynamics in more details we have fitted the data of $S''= 1/Y''$ in the crossover region where $\omega\tau_{\rm DW}(T) < 1 \rightarrow \omega\tau_{\rm DW}(T) > 1$ using a Cole-Cole relaxation, i.e.

$$S^*(\omega) = S_\infty + \frac{\Delta S^{\rm DW}}{1 + (i\omega\tau_{\rm DW})^{1-\alpha}} \qquad (4)$$

where S_∞ denotes the elastic compliance in the high frequency limit where $\omega\tau_{\rm DW} >> 1$ and $\Delta S^{\rm DW}$ refers to the DW-induced softening. The exponent $1-\alpha$ leads to a broadening (if $\alpha > 0$) of the Debye relaxation, which is obtained in the limit $\alpha = 0$. A Cole-Cole relaxation function fits the data quite well (Fig.5), yielding $\alpha \approx 0.8$.

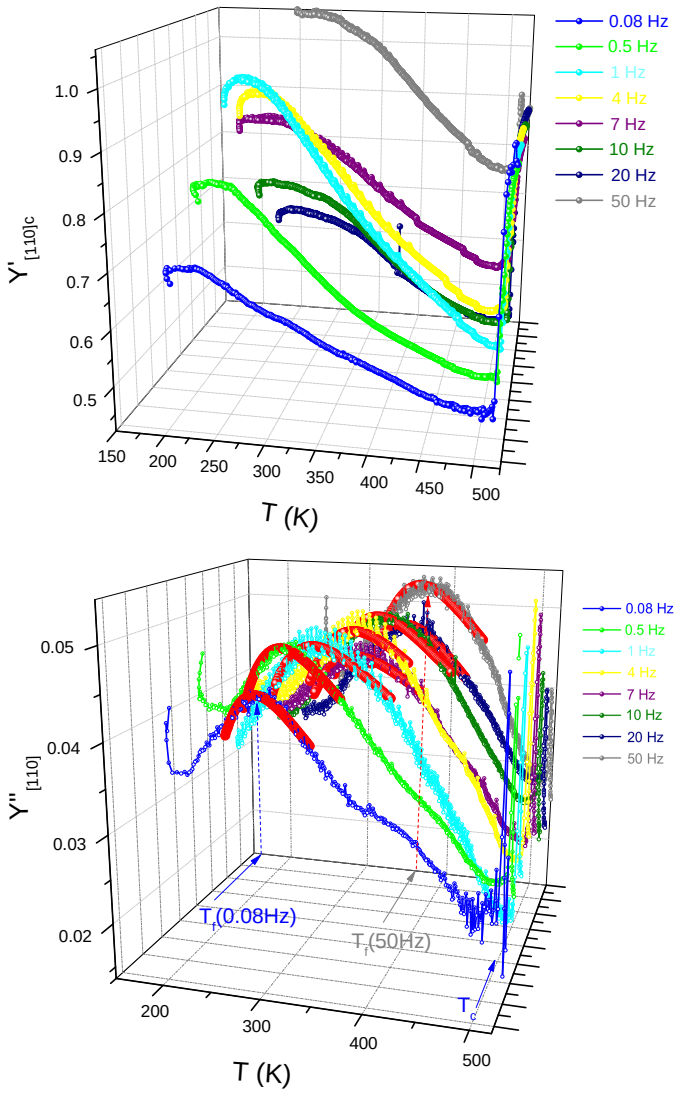

FIG. 5. Temperature dependencies of real and imaginary parts of Young's modulus of $PbZrO_3$ measured in $[110]_c$-direction at various frequencies. Red lines show Cole-Cole fits using Eq.4.

From these fits we extracted the temperature dependence of the relaxation time, shown in Fig.6.

It is evident that the temperature dependence of τ_{DW} deviates from a simple Arrhenius behaviour. It can be well fitted with a Vogel-Fulcher law

$$\tau_{\mathrm{DW}} = \tau_0 \; exp\left[\mathrm{E}/\mathrm{k_B}(\mathrm{T}-\mathrm{T_{VF}})\right] \qquad (5)$$

Various measurements in this crystal direction yielded similar relaxation behaviour of the DW freezing with fit parameters E=0.23 eV, $\tau_0 = 10^{-7} - 10^{-6}$s and $\mathrm{T_{VF}} = 120 \pm 10$ K.

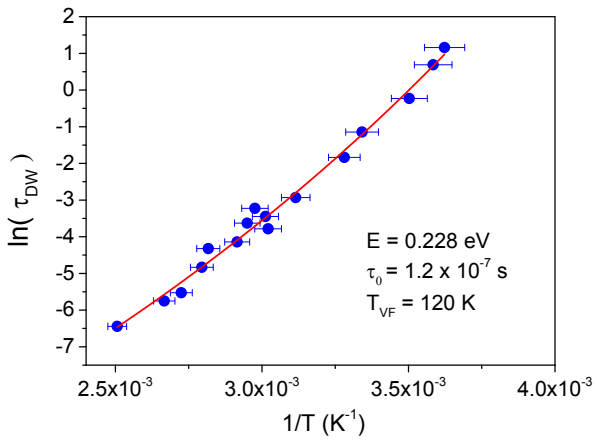

FIG. 6. Temperature dependence of the relaxation time τ_{DW} of domain wall motion plotted in semi-logarithmic scale.

B. Precursor dynamics

In all experiments where the effect of domain wall motion leads to a softening of the corresponding Young's modulus we observe quite interesting features in the high temperature cubic phase of $PbZrO_3$, never seen in any ferroic material before. Starting from about 60 K above $\mathrm{T_c}$ a hardening in Y′ occurs (instead of the precursor softening in $[100]_c$-direction), which is accompanied by a peak in Y″ (Fig.7). With decreasing frequency both anomalies shift to lower temperatures.
It seems evident that these high temperature anomalies are related to precursor clusters and we will discuss it in some details in the next section.

IV. DISCUSSION

We do not intend to calculate the measured elastic response of $PbZrO_3$ quantitatively. Our aim is to disentangle the various contributions which enter the dynamic elastic behaviour in different temperature regions. To get an idea of the expected intrinsic elastic anomalies we use the Landau free energy expansion given in Ref. 42. It turned out that the structural changes to the antiferroelectric phase in PZO cannot be completely described by one order parameter. An interplay of several modes is responsible for the symmetry breaking[29,30]. To describe the antiferroelectric phase in PZO the free energy consists at least of contributions from the following mode branches

$$F = F_0 + F_\Sigma + F_{\mathrm{R}} + F_{\Sigma\mathrm{R}} + F_{\varepsilon\Sigma\mathrm{R}} + F_\varepsilon \qquad (6)$$

where $\mathrm{F_0}$ is the background free energy of the cubic phase, F_Σ is written in invariants of order parameters (ρ_x, ρ_y, ρ_z) of the antiferroelectric Σ(TO)-mode, F_{R} in

terms of the R_{25}-mode order parameters (Φ_x, Φ_y, Φ_z), $F_{\Sigma R}$ describe couplings between Σ and R_{25}-mode, F_ε is the pure elastic energy and $F_{\varepsilon\Sigma R}$ includes the couplings between strains ε_i, Σ and R_{25}-mode. For a given orientational domain state of the orthorhombic phase, the displacement pattern can be described by a superposition of two lattice modes, i.e. $(\rho_x, \rho_y, \rho_z) = (0, 0, \rho(\mathbf{k}_\Sigma))$, with $\mathbf{k}_\Sigma = (2\pi/a_c)(1/4, 1/4, 0)$ describing mainly displacements of Pb-ions along y-direction and $(\Phi_x, \Phi_y, \Phi_z) = (\Phi(\mathbf{k}_R), \Phi(\mathbf{k}_R), 0)$ describes antiphase rotations of oxygen octahedra with $\mathbf{k}_R = (2\pi/a_c)(1/2, 1/2, 1/2)$, where a_c is the cubic lattice constant.
For a given domain state the various free energy contributions (6) are

$$
\begin{aligned}
F_\Sigma &= \frac{\alpha_\rho}{2}\rho^2 + \frac{\beta_\rho}{4}\rho^4 + \frac{\gamma_\rho}{6}\rho^6 \\
F_R &= \frac{\alpha_\Phi}{2}\Phi^2 + \frac{\beta_\Phi}{4}\Phi^4 + \frac{\gamma_\Phi}{6}\Phi^6 \\
F_{\Sigma R} &= \delta_\Phi \rho^2 \Phi^2 \\
F_{\varepsilon\Sigma R} &= \rho^2\{a_\rho(\varepsilon_1 + \varepsilon_2) + c_\rho\varepsilon_3\} + \Phi^2\{a_\Phi\varepsilon_1 + b_\Phi\varepsilon_2 + c_\Phi\varepsilon_3 + d_\Phi\varepsilon_6\} \\
F_\varepsilon &= \frac{C_{11}^0}{2}\left(\varepsilon_1^2 + \varepsilon_2^2 + \varepsilon_3^2\right) + C_{12}^0\left(\varepsilon_1\varepsilon_2 + \varepsilon_1\varepsilon_3 + \varepsilon_2\varepsilon_3\right) + \frac{C_{44}^0}{2}\left(\varepsilon_4^2 + \varepsilon_5^2 + \varepsilon_6^2\right)
\end{aligned}
\tag{7}
$$

In principle the condensation of the Σ- and R_{25}-modes are sufficient to describe the symmetry reduction into the *Pbam* space group, but there are several important experimental facts calling for a more complicated free energy expansion. First, to describe the observed Curie-Weiss type anomaly of the dielectric constant[43,44] in the paralectric phase, the free energy should in addition to (7) contain a contribution with respect to polarization P of the form

$$F_P = \frac{\alpha_\rho}{2}(T - T_F)P^2 + \delta_P P^2 \rho^2 \tag{8}$$

where the repulsive coupling $\delta_P > 0$ suppresses the Γ-point ferroelectric instability which would occur otherwise at T_F.
The condensation of the Σ-mode at $T_c \approx 510$ K would trigger the condensation of the R_{25}-mode due to the "Holakowsky" mechanism[45], i.e. the $\delta_\Phi\rho^2\Phi^2$-term in (7) with $\delta_\Phi < 0$. But the problem appeared that no critical softening was measured except for the Γ relaxational mode. To overcome this problem two quite different scenarios have been developed. Tagantsev, *et al.*[29] assumes that the antiferroelectric transition is driven by a flexoelectric coupling $f_{\alpha kl}(P_k \frac{\partial \varepsilon_\alpha}{\partial x_l} - \varepsilon_\alpha \frac{\partial P_k}{\partial x_l})$, which would induce an incommensurate phase with $\mathbf{k}$=k_0(1,1,0) that however is suppressed by strong "Umklapp -terms". In this picture the antiferroelectric phase of PZO is a "missed" incommensurate phase. In the model of Hlinka, *et al.*[30] it is assumed that the whole phonon branch related to Pb displacements softens, and a corresponding trilinear term triggers the AFE phase transition.
Both models are in some sense appealing and we should be aware of these complications with respect to the description of the AFE phase transition in PZO, when we try to disentangle the various contributions to the dynamic elastic anomalies. However, at the same time it is also clear that a quantitative analysis is very difficult due to the relatively large number of unknown model parameters which limits any quantitative analysis.
Fig.8 sketches the temperature dependence of the real and imaginary parts of Young's modulus to show the various contributions. The $\rho^2\varepsilon$- or $\Phi^2\varepsilon$-coupling terms in (7) are known to produce a negative dip anomaly (intrinsic anomaly in Fig.8) in the antiferroelectric phase for a sixth order expansion of the free energy[52]. As shown in Fig.4 such an anomaly was indeed measured in the direction where domain walls do not contribute. It is known, that domain wall motion leads to an additional softening of the elastic constants in directions, where the applied stress can move the domain walls. The domain wall contribution to the Young's modulus (Fig.8) can be most conveniently calculated[46,47] for the compliance S=1/Y as

$$\Delta S^{DW} \propto N_w \varepsilon_s^2 d_w^2 e^{x_0/d_w} \frac{1}{1 + (i\omega\tau_{DW})^{1-\alpha}} \tag{9}$$

where N_w is the number of domain walls, x_0 the average domain width, d_w is the domain boundary thickness and ε_s the spontaneous strain, which due to the quadratic-linear order parameter-strain coupling in Eq.(7) is proportional to the square of the order parameter[28]. Here a Cole-Cole type response for the domain wall relaxation is assumed with a T-dependent domain wall relaxation time τ_{DW}. In principle all terms in Eq.(9) can depend on temperature and without detailed knowledge of the temperature dependence of e.g. the domain wall width d_w(T) or the number of domain walls the temperature dependence of $\Delta S^{DW}(T)$ can only be estimated semi-quantitatively. Let us look at the various terms in Eq.(9). Electron Microscopy studies[48] revealed a small domain wall thickness of the order of unit cell dimensions. Thus d_w(T) is not expected to

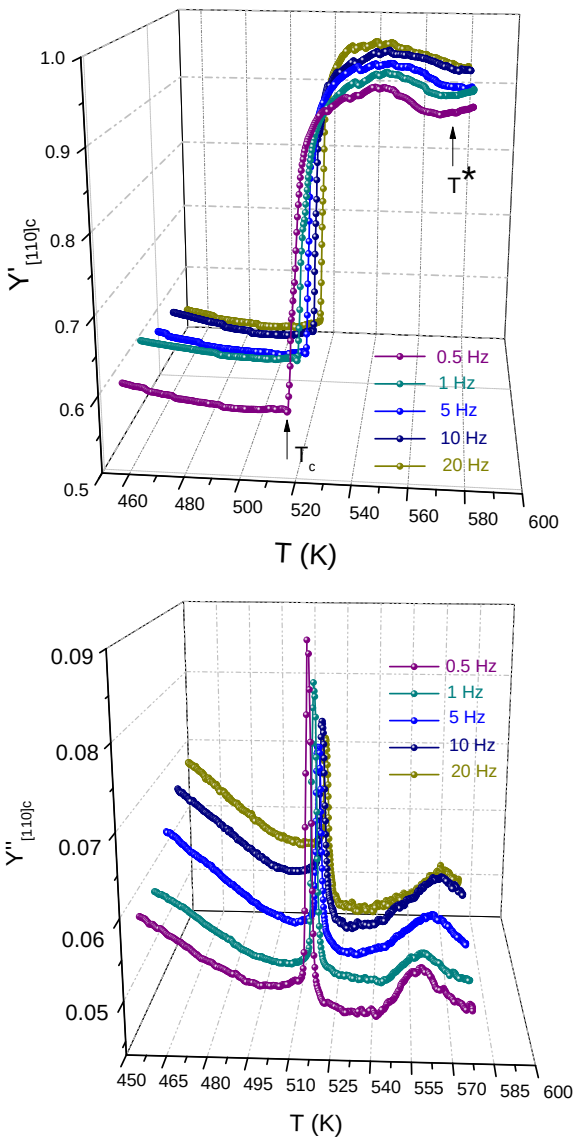

FIG. 7. Temperature dependencies of real and imaginary parts of Young's modulus of $PbZrO_3$ measured in $[110]_c$-direction at various frequencies. The plot region is changed with respect to Fig.5 to focus on the high temperature region.

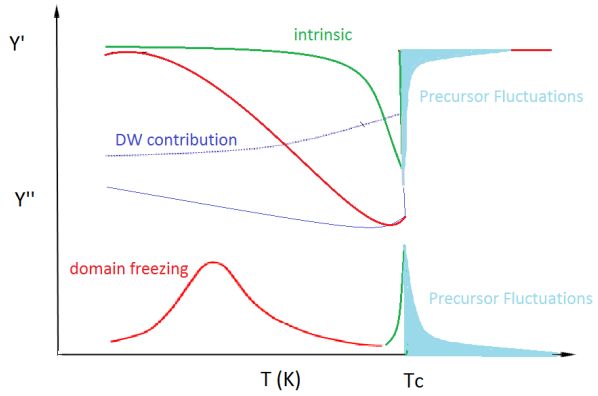

FIG. 8. Sketch of the different contributions to the overall elastic anomalies in $PbZrO_3$.

play an important role in Eq.9. By the way, in the frame of Landau-Ginzburg theory, thin domain walls would fit quite well into the picture of a flat phonon branch[30]. To study possible variations of the domain wall density with temperature we inspected the samples using a polarizing microscope (AXIOPHOT, ZEISS) and a heating/cooling chamber (THMS600, LINKAM), with no remarkable temperature dependence of N_w. We thus expect the main temperature dependence in Eq.(9) to come from the square of the spontaneous strain, implying $\Delta S^{\rm DW} \propto \Phi(T)^4 + \rho(T)^4$, sketched by the blue dashed line in Fig.8. With decreasing temperature the domain wall relaxation time $\tau_{\rm DW}$ increases and the domain walls can no longer follow the dynamical stress, i.e. they are frozen. A simultaneous fit of Y'' for different frequencies (Fig.5) yields a Vogel-Fulcher temperature dependence of the relaxation time (Fig. 6). This implies that "domain freezing" in $PbZrO_3$ is most probably a collective process, quite similar to glass forming liquids[49] or polymers[50].

Attention should also be paid to the observed deviations from mean-field elastic behaviour. Fig.4 shows that the Young's modulus decreases when the transition point of the cubic-orthorhombic transformation is approached from above. Such precursor softening of longitudinal elastic constants were previously reported for many perovskites, including $PbZrO_3$[37], $PbZr_{0.78}Sn_{0.22}O_3$[51], $PbHfO_3$[35] and $BaTiO_3$[38], etc. Using Landau-Ginzburg theory the fluctuation correction to the elastic susceptibility can be calculated[52,53] as

$$\Delta C^{\rm fl}(q=0,\omega) = \frac{2k_BT}{(2\pi)^3}a^3 \int \frac{d^3k}{1+i\frac{\omega\tau}{2}}\chi^2(k,0) \qquad (10)$$

In this approach, the temperature dependence of $\Delta C^{\rm fl}$ depends mainly on the form of the susceptibility $\chi(k)$. For isotropic fluctuations, i.e. $\chi(k) = \chi(k=0)/(1+k^2\xi^2)$ one obtains a power-law in the so called "Ising-limit"

$$\Delta C^{\rm fl}(q=0,\omega) \propto -(T-T_0)^{-1/2} \qquad (11)$$

For the case of a ferroelectric soft mode, the polarization fluctuations are strongly suppressed in the direction of the spontaneous polarization and as a result the susceptibility becomes anisotropic[54], leading to logarithmic corrections. Depending on the temperature range one can expect a crossover[55] from Ising (power-law at $T \gg T_0 + T_K$) to dipolar (logarithmic at $T \ll T_0 + T_K$) behaviour at $T \approx T_0 + T_K$ as

$$\Delta C^{\rm fl} \propto log\{1 + [T_K(T-T_0)]^{-1/2}\} \qquad (12)$$

As already mentioned above, a rather complicated mode-coupling mechanism[29,30] drives the antiferroelec-

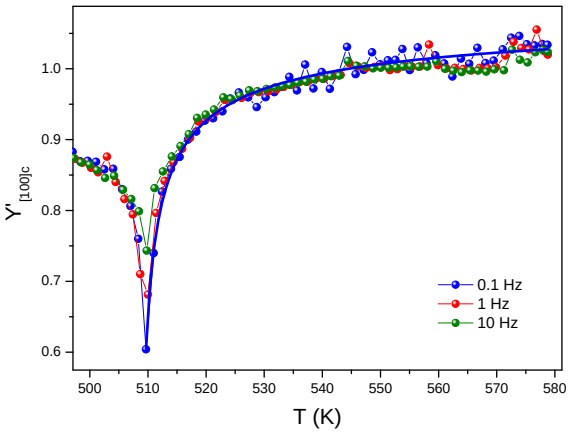

FIG. 9. Magnified view of the high temperature region of $Y'_{[100]c}$ to show the behaviour above T_c more clearly. The line is a fit using isotropic fluctuation corrections in mean-field approximation, yielding an exponent of $\frac{1}{2}$.

tric phase transition in $PbZrO_3$. Moreover, in the cubic phase a considerable amount of diffuse scattering is detected[56] at the M and R points of the Brillouin zone. The question on the behaviour of the fluctuation contributions is intimately connected with the type of coupling, because it finally determines the shape of the corresponding susceptibility in Eq.(10) and with it the T-dependence of $\Delta C^{\rm fl}$. This problem becomes even more transparent if we look at the more intensively investigated case of $BaTiO_3$. This material shows also elastic softening in a broad temperature range above T_c. Several models have been tried to explain this softening. Salje, *et al.*[38] have shown that a power-law Eq.(11) cannot fit the data at all. Instead they used a Vogel-Fulcher type temperature dependence to fit the elastic constant, $\Delta C^{fl} \propto exp[E_a/(T-T_{VF})]$. The Vogel-Fulcher temperature T_{VF}, turns out to be below the transition temperature and the activation energy, E_a, corresponds to the typical hopping energy of disordered Ti positions in $BaTiO_3$. The empirical observation of the large precursor softening and the corresponding glassy dynamics inspired the authors to the concept of "domain glass"[22]. This is a very appealing concept and Vogel-Fulcher type elastic softening was also observed in other systems, e.g. in $PbSc_0.5Ta_0.5O_3$(PST)[57]. Moreover, this concept may pave the way for a description of Relaxors. However, Ko, et al.[37] found logarithmic fluctuation corrections in $BaTiO_3$ to be valid in a broad temperature range of 80 K above T_c. Also in PST a power-law type fluctuation contribution fits the data well.

With this in mind we applied the above proposed models to our data. The best fits were obtained (Fig.9) for isotropic fluctuations (Eq.11) with a T_0 about 2 K below T_c. Since the non occurring ferroelectric phase transition temperature T_F is about 30 K below T_c it indicates that the precursor softening observed here in Y′ in

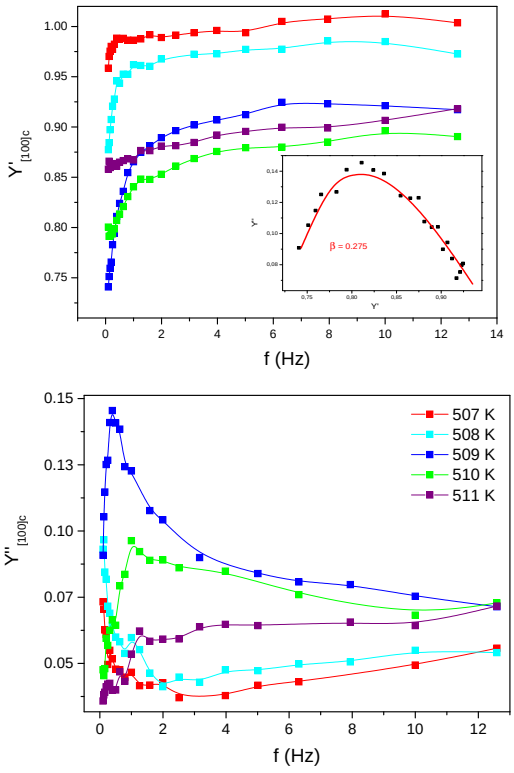

FIG. 10. Frequency scans revealing $Y'_{[100]c}$(f) and $Y''_{[100]c}$(f) in the vicinity of the antiferroelectric phase transition. The inset shows the Cole-Davidson behaviour of the relaxation at 509 K, yielding an exponent β=0.27.

the low frequency regime has its origin in fluctuations of order parameters corresponding to fluctuations in antiphase rotations $\Phi(\mathbf{k}_{\rm R})$ of oxygen octahedra or lead ion displacements $\rho(\mathbf{k}_{\Sigma})$ and not in polarization fluctuations $P(k=0)$. But this implies that the corresponding mode should also soften at T_0, i.e. α_Φ or α_ρ $\propto$(T-T_0), which would be in agreement with Hlinka's[30] scenario. The fact that we observe a peak in Y″ only in the close vicinity of T_c shows that the corresponding order parameter dynamics is too fast to be detected in the low frequency range, i.e. $\omega\tau_{\rho,\Phi} \ll 1$.

The detection of a strong peak in Y″ in the close vicinity of T_c together with a pronounced frequency dependence of the anomalies in Y′ and Y″ indicate that the corresponding dynamic process is on the time scale of $\tau > 1/2\pi f$, where f=0.1-10 Hz. Detailed frequency scans of Y′ and Y″ in the close vicinity of T_c revealed a non-Debye behaviour (Fig.10), that can be fitted with a Cole-Davidson type relaxation function. A possible origin of this low frequency relaxation is heat diffusion[59], which leads to a crossover from isothermal ($\omega\tau_{th} < 1$) elastic behaviour to adiabatic one ($\omega\tau_{th} > 1$) at $\omega\tau_{th} \approx 1$

$$c^{-1}_{\mu\nu}(\omega) = c^{-1\ S}_{\mu\nu} - \frac{T\alpha_\mu\alpha_\nu}{C_p}\Omega(\omega\tau_{th}) \qquad (13)$$

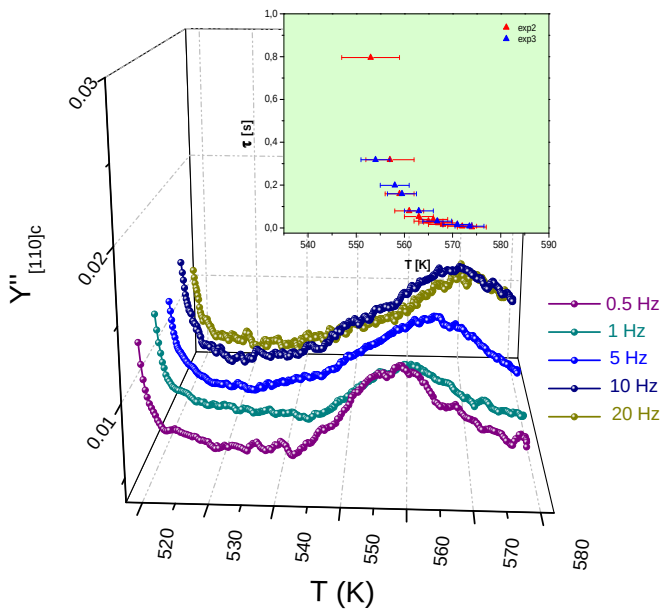

FIG. 11. $Y''_{[110]c}$ in the precursor region above T_c together with the temperature dependence of the relaxation time τ calculated from the positions of the peak maxima.

where Voigt notation is used, α_μ is the thermal expansion coefficient, C_p the specific heat and $\tau_{th} = 1/Dq^2$ is the characteristic thermal diffusion time, i.e. the time needed to transfer heat over a distance of $d = 2\pi/q$, where d is the size of the sample. For a typical sample size of few mm $\tau_{th} \approx$ 1s, in good agreement with our findings (Fig.10). The specific form of the function $\Omega(\omega\tau_{th})$ describing the crossover between isothermal and adiabatic behaviour depends generally on the boundary conditions, but as was shown[61] for elastic measurements of monodomain samples in parallel plate and three point bending geometry to be a Debye-like function. For heat diffusion in polydomain crystals and heterogeneous systems one expects dispersions of a non-Debye type. Thus it seems likely that the low frequency relaxation process observed here in the very close vicinity of T_c originates from an isothermal - adiabatic crossover, which is strongest (Eq.13) at T_c[12,60], where the thermal expansion coefficients are largest.

Finally let's discuss the dynamic hardening observed in $Y'_{[110]c}$ in the paraelectric phase of $PbZrO_3$, which is accompanied by a distinct peak in Y'' (Fig.7). Interestingly, the effect starts around 60 K above T_c, very similar to the onset of birefringence and piezoelectric coefficient d_{11}, recently detected[37] in $PbZrO_3$. Ko, *et al.* relate these observations which apparently disagree with cubic symmetry to the presence of large polar clusters. They however did not exclude the possibility that the symmetry breaking may be due to some strains and other static defects in the crystal. We think that our observation of the pronounced dynamic stiffening (Fig.7, Fig.3) is related to the onset of dynamic polar clusters which increase in size with decreasing temperature. Phenomenologically the effect can be described by taking into account the difference between the elastic constants at constant electric field $C^E_{\mu\nu}$ and constant polarization $C^P_{\mu\nu}$ as[25]

$$C^{-1\ P}_{\mu\nu} = C^{-1\ E}_{\mu\nu} - d_{j\mu} d_{l\nu} \epsilon^{-1}_{lj} \qquad (14)$$
$$j = 1-3; \mu = 1-6$$

Eq.14 explains how the observed hardening in $Y'_{[110]c}$ may be related to the piezoelectric anomaly[37]. According to Eq.14 polarization fluctuations lower the elastic constant, since $C^P_{\mu\nu} > C^E_{\mu\nu}$ and thus $Y^P > Y^E$. With decreasing temperature the relaxation time τ increases rather strongly and we observe a crossover between Y^P and Y^E at a temperature where $\omega\tau \approx 1$ leading to the observed hardening in Y' as well as the peak in Y'' above T_c. From the peculiar anisotropy of this effect, which we observe only in [110]-direction, we infer that it is probably a result of the strong flexoelectric coupling[29] which induces polarization fluctuations via strain gradients that are present in the sample as ferroelastic precursors[62]. As was shown theoretically[32] for $PbZrO_3$, elastic and polar precursors start to develop more than 100 K above T_c whose spatial extent increases, reaching more than 10 nm at T_c. Quite recently, Salje, *et al.*[63] demonstrated some close links between different ferroelastic twin pattern and electrical polarization via flexoelectric coupling, using an atomistic toy model and continuum theory, which may be used in future to explain such precursor effects. It should be noted that the relaxation time τ increases very rapidly with decreasing temperature (Fig. 11) and seems to diverge at a temperature considerably higher than T_c. However, without a detailed model no definite conclusions can be drawn here. Nevertheless, it is obvious that the dynamic nature of this effect rules out any kinds of static defects to be responsible for it.

V. CONCLUSION

The paraelectric to antiferroelectric phase transition in $PbZrO_3$ is anything but simple[64] and several mode coupling schemes[29,30,32,65] have been proposed to describe all structural distortions of the orthorhombic phase. It is far beyond the scope of this paper to fit our data quantitatively and discriminate between different models, but we used them to disentangle the various contributions to the low frequency elastic constants of $PbZrO_3$. The main results are:

(1) For dynamic forces that are applied in the direction parallel or perpendicular to the domain walls, the elastic response (Fig.4) reflects the intrinsic behaviour. The observed anomalies, i.e. a cusp in $Y'_{[100]c}$ and a peak in $Y''_{[100]c}$ at T_c are due to a quadratic-linear coupling between order parameter and strain, where most probably all order parameters

that are active in the transition (lead displacements + oxygen octahedra rotations) contribute. The fact, that the anomaly in Y' is cusp-like instead of a negative step shows that the Landau free energy should be expanded up to at least sixth order in the corresponding order parameters.

(2) The observed precursor softening in this direction can be perfectly fitted with a power-law $\Delta Y'^{(fl)}_{[100]c} \propto (T - T_0)^{-1/2}$ originating from isotropic fluctuations. Since T_0 is only slightly (one or two K) below T_c these fluctuation contributions stem from fluctuations in ρ and/or Φ, rather than from polarization fluctuations. This is in agreement with the scenario of Hlinka, *et al.*[30] who proposed a softening of the whole polarization branch, which was experimentally proved by Burkovsky, *et al.*[?] .

(3) In directions 45° with respect to domain walls some signatures of polar clusters are found. Depending on measurement frequency, at approximately 60 K above T_c the Young's modulus starts to increase with decreasing temperature, before it drops down at T_c. The corresponding imaginary part in Y'' shows a distinct maximum, shifting to lower T with decreasing frequency. The relaxation time of this process increases with decreasing temperature by two orders of magnitude within a 20 K interval, indicating that the movement of the polar regions considerably slows down. We are not aware of any other observation of such a dynamic hardening, and a comprehensive model to explain this behaviour is still missing. We tentatively describe the effect to be due to a crossover between $C^{-1\ E}_{\mu\nu}$ and $C^{-1\ P}_{\mu\nu}$, whose difference is determined by the ratio of piezoelectric coefficients and dielectric permittivity. In fact it was shown[37] that the piezoelectric coefficient d_{11} starts to increase from zero to finite values at about T_c+50 K. At the same temperature a clear onset of birefringence was observed in $PbZrO_3$. Similar precursor behaviour was found in $BaTiO_3$ in birefringence and central peak intensity[58], which most probably are all related to the onset of polar clusters[33,67] at a temperature $T^* \approx 1.1$ T_c. From the dynamic nature of the observed elastic hardening we conclude that this is not an effect of defects that break the symmetry statically, but the polar clusters are an intrinsic dynamic effect of the material.

(4) Below T_c, i.e. in the antiferroelectric phase of $PbZrO_3$ we have detected an additional contribution to the elastic behaviour, which is due to domain wall motion. This additional softening disappears gradually with decreasing temperature. The domain wall dynamics shows up in the imaginary part of the complex Young's modulus, which displays a peak around the domain freezing temperature. From a detailed analysis of this peak and its shift with frequency we have determined the domain wall relaxation time τ_{DW}. It follows a Vogel-Fulcher temperature dependence with $T_{VF} \approx 120$ K, which is considerably far below T_c. This implies, that the domain freezing in lead zirconate bears some similarities to glass freezing. Although recent large scale computer simulations[22] on similar systems with ferroelastic domain walls gave valuable insights into the physics of domain freezing, up to now it is not clear what mechanism leads to the Vogel-Fulcher type relaxation. In glass-forming liquids[68] it seems settled that the diverging relaxation time at finite temperature (T_{VF}) is due to the presence of dynamically correlated regions whose size ξ increases, reaching infinity at T_{VF}. It is a big challenge to look for such dynamical correlations in systems with domain freezing. The present study shows that Lead Zirconate is a good candidate for this purpose.

VI. ACKNOWLEDGMENTS

The present work was supported by the Austrian Science Fund (FWF) Grant No. P28672-N36.

* sabine.puchberger@univie.ac.at
† wilfried.schranz@univie.ac.at

[1] J. Fousek, D.B. Litvin and L.E. Cross, J. Phys.: Condens. Matter **13**, L33 - L38 (2001).
[2] D.D. Viehland and E.K.H. Salje, Adv. Phys. **63**, 267 - 326 (2014).
[3] Y. Jin, Y. Wang, A. Khachaturyan, J.F. Li, and D. Viehland, J. Appl. Phys. **94**, 3629 - 3640 (2003).
[4] G. Busch and P. Scherrer, Naturwissenschaften **23**, 737 (1935).
[5] C. Kittel, Phys. Rev. **83**, 458 (1951).
[6] A.K. Tagantsev, L.E. Cross and J. Fousek, *Domains in Ferroic Crystals and Thin Films*, Springer LLC 2010.
[7] A. Sidorkin, Ferroelectrics, **191**, 109 - 128 (1997).
[8] J. Bornarel and B. Torche, Ferroelectrics **132**, 273 - 283 (1992).
[9] Y. Huang, X. Li, Y. Ding, H. Shen, Z.F. Zhang, Y.N. Wang, C.S. Fang and S.H. Zhu, Journal de Physique IV Colloque, **6** (C8), 815 - 818 (1996).
[10] A.V. Kityk, W. Schranz, P.Sondergeld, D. Havlik, E.K.H. Salje and J.F. Scott, Phys. Rev. B **61**, 946 (2000).
[11] A.V. Kityk, W. Schranz, P.Sondergeld, D. Havlik, E.K.H. Salje and J.F. Scott, Europhysics Letters **50**, 41-47 (2000).
[12] W. Schranz, A. Tröster, A.V.Kityk, P. Sondergeld and E.K.H. Salje, Europhys. Letters **62**, 512 (2003).
[13] W. Schranz, P. Sondergeld, A. V. Kityk, and E. K. H. Salje, Phys. Rev. B **80**, 094110 (2009).

[14] R.J. Harrison, S.A.T. Redfern and J. Street, Am. Min. **88**, 574 (2003).
[15] R.J. Harrison and S.A.T. Redfern, Phys. Earth Planet. Interiors **134**, 253 (2002).
[16] Y. Wang, W. Sun, X. Chen, H. Shen, and B. Lu, Phys. Status Solidi A **102**, 279 (1987).
[17] Y.N. Huang, X. Li, Y. Ding, Y.N. Wang, H.M. Shen, Z.F. Zhang, C.S. Fang, S.H. Zhuo and P.C.W. Fung, Phys. Rev. B **55**, 16159 (1997).
[18] J. Kumar and A.M. Awasthi, Appl. Phys. Lett. **103**, 132903 (2013).
[19] X. Ren, Y. Wang, K. Otsuka, P. Lloveras, T. Castán, M. Porta, A. Planes and A. Saxena, MRS Bull. **34**, 838 (2009).
[20] X. Ren, Phys. Stat. Sol. B **251**, 1982 (2014).
[21] S. Kustov, D. Salas, E. Cesari, R. Santamarta, D. Mariand J. Van Humbeeck, Acta Materialia **73**, 275 (2014).
[22] E.K.H. Salje, X. Ding and O. Atkas, Phys. Stat. Sol. B **251**, 2061 (2014).
[23] E.K.H. Salje, X. Ding,Z. Zhao,T. Lookman and A. Saxena, Phys. Rev. B **83**, 104109 (2011).
[24] S. Roberts, J. Am. Ceram. Soc. **33**, 63 (1950).
[25] M.E. Lines, A.M. Glass. *Principles and applications of ferroelectrics*. Oxford: Clarendon Press; 1977
[26] A.M. Glazer, K. Roleder, J. Dec, Acta Cryst. B **49**,846 (1993).
[27] N. Zhang, H. Yokota, A.M. Glazer and P.A. Thomas, Acta Cryst. B **67**, 461 (2011).
[28] H. Fujishita, Y. Shiozaki, N. Achiva, E. Sawaguchi, J. Phys Soc. Jpn. **51**, 3583 (1982).
[29] A.K. Tagantsev, K. Vaideeswaran, S.B. Vakhrushev, A.V. Filimonov, R.G. Burkovsky, A. Shaganov, D. Andronikova, A.I. Rudskoy, A.Q.R. Baron, H. Uchiyama, D. Chernyshov, A. Bosak, Z. Ujma, K. Roleder, A. Majchrowski, J.H. Ko, N. Setter, Nature Commun. **4**, 2229(1-8), (2013).
[30] J. Hlinka, T. Ostapchuk, E. Buixaderas, C. Kadlec, P. Kuzel, I. Gregora, J. Kroupa, M. Savinov, A. Klic, J. Drahokoupil, I. Etxebarria and J. Dec, Phys. Rev. Lett. **112**, 197601 (2014).
[31] G. Kugel, I. Jankowska-Sumara, K. Roleder and J. Dec, J. Korean Phys. Soc. **32**, S581 (1998).
[32] A. Bussmann-Holder, J.-H. Ko, A. Majchrowski, M. Górny and K. Roleder, J. Phys.: Condens. Matter **25**, 212202 (2013).
[33] A. Bussmann-Holder, H. Beige and G. Volkel, Phys. Rev. B **79**, 184111 (2009).
[34] K. Roleder, A. Bussmann-Holder, M. Górny, K. Szot and A.M. Glazer, Phase Transit. **85**, 939 (2012).
[35] A. Bussmann-Holder, T.H. Kim, B.W. Lee, J.-H. Ko, A. Majchrowski, A. Soszyński and K. Roleder, J. Phys.: Condens. Matter **27**, 105901 (2015).
[36] T.H. Kim, S. Kojima, K. Park, S.B. Kim and J.-H. Ko, J. Phys.: Condens. Matter **22**, 225904 (2010).
[37] J.-H. Ko, M. Górny, A. Majchrowski, K. Roleder and A. Bussmann-Holder, Phys. Rev. B **87**, 184110 (2013).
[38] E.K.H. Salje, M.A. Carpenter, G.F. Nataf, G. Picht, K. Webber, J. Weerasinghe, S. Lisenkov and L. Bellaiche, Phys. Rev. B **87**, 014106 (2013).
[39] J.-Ko., K. Roleder and A. Bussmann Holder, IOP Confer. Ser.: Materials Science and Eng. **54**, 012002 (2014).
[40] W. Schranz, Phase Transit. **64**, 103 (1997).
[41] E.K.H. Salje and W. Schranz, Z. Kristallographie **226**, 1 (2011).
[42] H. Fujishita, Y. Ishikawa, S. Tanaka, A. Ogawaguchi and S. Katano, J. Phys. Soc. Jpn. **72**, 1426 (2003).
[43] G. Shirane, E. Sawaguchi and Y. Takagi, Phys. Rev. **84**, 476 (1951).
[44] D. Viehland, Phys. Rev. B **52**, 778 (1995).
[45] J. Holakowsky, Phys. Status Solidi (b) **56**, 615 (1973).
[46] W. Schranz, H. Kabelka, A. Sarras and M. Burock, Appl. Phys. Lett. **101**, 141913 (2012).
[47] W. Schranz, Phys. Rev. B **83**, 094120 (2011).
[48] M. Tanaka, R. Saito and K. Tsuzuki, Jpn. J. Appl. Phys. **21**, 291 (1982).
[49] J. Koppensteiner, W. Schranz and M.A. Carpenter, Phys. Rev. B **81**, 024202 (2010).
[50] M. Reinecker, V. Soprunyuk, M. Fally, A. Sánchez-Ferrer and W. Schranz, Soft Matter **10**, 5729 (2014).
[51] M. Maczka, T.H. Kim, M. Ptak, J. Jankowska-Sumara, A. Majchrowski and S. Kojima, J. Alloys and Comounds, **587**, 273 (2014).
[52] W. Rehwald, Adv. Phys. **22**, 721 (1973).
[53] W. Schranz, M. Fally and D. Havlik, Phase Transitions **65**, 27 (1998).
[54] A.P. Levanyuk, K.A. Minaeva and B.A. Strukov, Sov. Phys.-Solid State **10**, 1919 (1969).
[55] P. Kubinec, W. Schranz and H. Kabelka, J. Phys.: Condens. Matter **4**, 7009 (1992).
[56] N. Zhang, M. Pásciak, A. M. Glazer, J. Hlinka, M. Gutmann, H. A. Sparkes, T. R. Welberry, A. Majchrowski, K. Roleder, Y. Xie and Z.-G. Ye, J. Appl. Cryst. **48**, 1637 (2015).
[57] O. Aktas, E.K.H. Salje, S. Crossley, G. I. Lampronti, R. W. Whatmore, N. D. Mathur, and M. A. Carpenter, Phys. Rev. B **88**, 174112 (2013).
[58] J.-H. Ko, T. H. Kim, K. Roleder, D. Rytz and S. Kojima, Phys. Rev. B **84**, 094123 (2011).
[59] W. Schranz and D. Havlik, Phys. Rev. Lett. **73**, 2575 (1994).
[60] K. Hamano and K. Ema, J. Phys. Soc. Jpn. **45**(3), 923 (1978).
[61] A.Tröster and W. Schranz, Phys. Rev. B **66**, 184110 (2002).
[62] Z. Zhao, X. Ding and E.K.H. Salje, Appl. Phys. Lett. **105**, 112906 (2014).
[63] E.K.H. Salje, S. Li, M. Stengel, P. Gumbsch and X. Ding, Phys. Rev. B **94**, 024114 (2016).
[64] P. Tolédano and M. Guennou, Phys. Rev. B **94**, 014107 (2016).
[65] J. Íñiguez, M. Stengel, S. Prosandeev and L. Bellaiche, Phys. Rev. B **90**, 220103 (2014).
[66] R. G. Burkovsky, A. K. Tagantsev, K. Vaideeswaran, N. Setter, S. B. Vakhrushev, A. V. Filimonov, A. Shaganov, D. Andronikova, A. I. Rudskoy, A. Q. R. Baron, H. Uchiyama, D. Chernyshov, Z. Ujma, K. Roleder, A. Majchrowski, and Jae-Hyeon Ko, Phys. Rev. B **90**, 144301 (2014).
[67] A. Zibińska, D. Rytz, K. Szot, M. Górny and K. Roleder, J.Phys.: Condens. Matter **20**, 142202, (2008).
[68] B. Rijal, L. Delbreilh and A. Saiter, Macromolecules **48**, 8219 (2015).